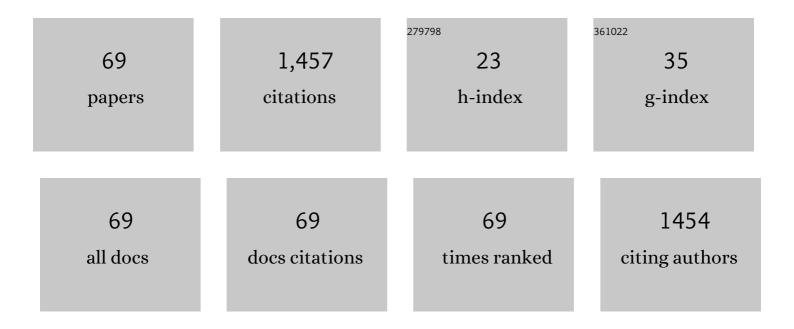


List of Publications by Year in descending order

Source: https://exaly.com/author-pdf/4177777/publications.pdf Version: 2024-02-01



ΒΛΝΙΙΛ

#	Article	IF	CITATIONS
1	Novel 2D boron nitride with optimal direct band gap: A theoretical prediction. Applied Surface Science, 2022, 578, 151929.	6.1	19
2	Comparative <i>ab initio</i> calculations of SrTiO3, BaTiO3, PbTiO3, and SrZrO3 (001) and (111) surfaces as well as oxygen vacancies. Low Temperature Physics, 2022, 48, 80-88.	0.6	4
3	Online Wear Particle Detection Sensors for Wear Monitoring of Mechanical Equipment—A Review. IEEE Sensors Journal, 2022, 22, 2930-2947.	4.7	26
4	Edge modified phosphorene nanoribbon heterojunctions: promising metal-free photocatalysts for direct overall water splitting. Journal of Materials Science, 2022, 57, 5482-5496.	3.7	6
5	Carbon ene-yne working in oxygenator: A theoretical study. Diamond and Related Materials, 2022, 125, 108991.	3.9	4
6	How does fluoride enhance hydroxyapatite? A theoretical understanding. Applied Surface Science, 2022, 586, 152753.	6.1	7
7	Penta-silicon carbide: A theoretical investigation. Materials Science and Engineering B: Solid-State Materials for Advanced Technology, 2022, 281, 115740.	3.5	1
8	Ab Initio Computations of O and AO as well as ReO2, WO2 and BO2-Terminated ReO3, WO3, BaTiO3, SrTiO3 and BaZrO3 (001) Surfaces. Symmetry, 2022, 14, 1050.	2.2	23
9	Theoretical investigations of the heavily boron doped pentadiamond. Diamond and Related Materials, 2022, 126, 109127.	3.9	1
10	B N counterpart of biphenylene network: A theoretical investigation. Applied Surface Science, 2022, 598, 153674.	6.1	18
11	Molecular Dynamics Simulation Investigation of the Binding and Interaction of the EphA6–Odin Protein Complex. Journal of Physical Chemistry B, 2022, 126, 4914-4924.	2.6	7
12	Overall direct photocatalytic water-splitting on <i>C</i> 2 <i>mm</i> -graphyne: a novel two-dimensional carbon allotrope. Journal of Materials Chemistry C, 2022, 10, 10843-10852.	5.5	13
13	Study on the Sensitivity of Detachable Wear Particle Sensor Based on Iron-Based Amorphous Soft Magnetic Rings. IEEE Sensors Journal, 2022, 22, 12708-12718.	4.7	3
14	Theoretical investigation of the influence of different electric field directions and strengths on a POM-based dye for dye-sensitized solar cells. Materials Chemistry Frontiers, 2021, 5, 929-936.	5.9	2
15	Synthesis of MoSe ₂ /CoSe ₂ Nanosheets for NIRâ€Enhanced Chemodynamic Therapy via Synergistic Inâ€5itu H ₂ O ₂ Production and Activation. Advanced Functional Materials, 2021, 31, 2008420.	14.9	59
16	DFT and TDDFT Studies of Non-Fullerene Organometallic Based Acceptors for Organic Photovoltaics. Journal of Inorganic and Organometallic Polymers and Materials, 2021, 31, 1676-1687.	3.7	6
17	NIR-Driven Intracellular Photocatalytic O ₂ Evolution on Z-Scheme Ni ₃ S ₂ /Cu _{1.8} S@HA for Hypoxic Tumor Therapy. ACS Applied Materials & Interfaces, 2021, 13, 9604-9619.	8.0	50
18	Comparative Hybrid Hartree-Fock-DFT Calculations of WO2-Terminated Cubic WO3 as Well as SrTiO3, BaTiO3, PbTiO3 and CaTiO3 (001) Surfaces. Crystals, 2021, 11, 455.	2.2	44

Ran Jia

#	Article	IF	CITATIONS
19	Dipoles in 4,12,4-graphyne. Applied Surface Science, 2021, 545, 148991.	6.1	12
20	Fabrication of three-component hydrogen-bonded covalent-organic polymers for ciprofloxacin decontamination from water: adsorption mechanism and modeling. Materials Today Chemistry, 2021, 20, 100463.	3.5	5
21	Metal doped fullerene complexes as promising drug delivery materials against COVID-19. Chemical Papers, 2021, 75, 6487-6497.	2.2	19
22	Pathway of in situ polymerization of 1,3-dioxolane in LiPF6 electrolyte on Li metal anode. Materials Today Energy, 2021, 21, 100730.	4.7	22
23	Metallic subnanometer porous silicon: A theoretical prediction. Physical Review B, 2021, 103, .	3.2	13
24	The molecular mechanism behind protein kinase B natural mutant E17K affecting the allosteric inhibitor sensitivity: a molecular dynamics simulation study. Journal of Biomolecular Structure and Dynamics, 2021, 39, 1-14.	3.5	9
25	Tendencies in ABO3 Perovskite and SrF2, BaF2 and CaF2 Bulk and Surface F-Center Ab Initio Computations at High Symmetry Cubic Structure. Symmetry, 2021, 13, 1920.	2.2	30
26	Comparative Hybrid Hartree-Fock-DFT Calculations of ReO ₃ , SrTiO ₃ , BaTiO ₃ , PbTiO ₃ and CaTiO ₃ (001) Surfaces. Integrated Ferroelectrics, 2021, 220, 9-17.	0.7	3
27	Ab initio calculations of CaZrO3 (011) surfaces: systematic trends in polar (011) surface calculations of ABO3 perovskites. Journal of Materials Science, 2020, 55, 203-217.	3.7	23
28	Giant piezoelectricity in B/N doped 4,12,2-graphyne. Applied Surface Science, 2020, 499, 143800.	6.1	18
29	How does the porphyrin-like vacancy affect the spectral properties of graphene quantum dots? A theoretical study. Journal of Physics Condensed Matter, 2020, 32, 155902.	1.8	4
30	Frontispiz: Subnanometer Bimetallic Platinum–Zinc Clusters in Zeolites for Propane Dehydrogenation. Angewandte Chemie, 2020, 132, .	2.0	0
31	Comparative Ab Initio Calculations of ReO3, SrZrO3, BaZrO3, PbZrO3 and CaZrO3 (001) Surfaces. Crystals, 2020, 10, 745.	2.2	46
32	Assembly of polysubstituted chiral cyclopropylamines <i>via</i> highly enantioselective Cu-catalyzed three-component cyclopropene alkenylamination. Chemical Communications, 2020, 56, 12250-12253.	4.1	11
33	Frontispiece: Subnanometer Bimetallic Platinum–Zinc Clusters in Zeolites for Propane Dehydrogenation. Angewandte Chemie - International Edition, 2020, 59, .	13.8	5
34	Co-doping with boron and nitrogen impurities in T-carbon. Journal of Saudi Chemical Society, 2020, 24, 857-864.	5.2	5
35	Studies on covalent functionalization of single layer black phosphorus from GW calculations based on the many body perturbation theory. Electronic Structure, 2020, 2, 025005.	2.8	5
36	Configuration effect in polyoxometalate-based dyes on the performance of DSSCs: an insight from a theoretical perspective. Physical Chemistry Chemical Physics, 2020, 22, 16032-16039.	2.8	3

Ran Jia

#	Article	IF	CITATIONS
37	Subnanometer Bimetallic Platinum–Zinc Clusters in Zeolites for Propane Dehydrogenation. Angewandte Chemie - International Edition, 2020, 59, 19450-19459.	13.8	221
38	Arranging strategies for A-site cations: impact on the stability and carrier migration of hybrid perovskite materials. Inorganic Chemistry Frontiers, 2020, 7, 1741-1749.	6.0	17
39	A novel T-C ₃ N and seawater desalination. Nanoscale, 2020, 12, 5055-5066.	5.6	26
40	Subnanometer Bimetallic Platinum–Zinc Clusters in Zeolites for Propane Dehydrogenation. Angewandte Chemie, 2020, 132, 19618-19627.	2.0	47
41	Iron oxides with a reverse spinel structure: impact of active sites on molecule adsorption. Inorganic Chemistry Frontiers, 2019, 6, 2810-2816.	6.0	12
42	Computational and biological investigation of the soybean lecithin–gallic acid complex for ameliorating alcoholic liver disease in mice with iron overload. Food and Function, 2019, 10, 5203-5214.	4.6	14
43	Theoretical study on the influence of electric field direction on the photovoltaic performance of aryl amine organic dyes for dye-sensitized solar cells. New Journal of Chemistry, 2019, 43, 651-661.	2.8	7
44	How does graphene enhance the photoelectric conversion efficiency of dye sensitized solar cells? An insight from a theoretical perspective. Journal of Materials Chemistry A, 2019, 7, 2730-2740.	10.3	26
45	Regulating vibrational modes to improve quantum efficiency: insights from theoretical calculations on iridium(<scp>iii</scp>) complexes bearing tridentate NCN and NNC chelates. Dalton Transactions, 2019, 48, 5064-5071.	3.3	9
46	Designation and Match of Nonâ€Fullerene Acceptors with Xâ€Shaped Donors toward Organic Solar Cells. ChemistrySelect, 2019, 4, 3654-3664.	1.5	10
47	Nickel-catalyzed carboxylation of aryl zinc reagent with CO2: A theoretical and experimental study. Journal of CO2 Utilization, 2019, 29, 262-270.	6.8	3
48	Investigating detailed mechanism of hydrogen molecules adsorbing on singleâ€wall carbon nanotubes using fitted force field parameters containing carbon–carbon interactions. Journal of Computational Chemistry, 2019, 40, 1073-1083.	3.3	0
49	Origin of the deep band-gap state in <mmi:math xmlns:mml="http://www.w3.org/1998/Math/MathML"> <mmi:msub> <mmi:mi>TiO </mmi:mi> <mmi:mn>2 (110): <mmi:math xmlns:mml="http://www.w3.org/1998/Math/MathML"> <mmi:mrow> <mmi:mi>d </mmi:mi> <mmi:mi>d </mmi:mi></mmi:mrow></mmi:math </mmi:mn></mmi:msub></mmi:math 	3.2	14
50	Comprehensive Investigation into Luminescent Properties of Ir(III) Complexes: An Integrated Computational Study of Radiative and Nonradiative Decay Processes. Inorganic Chemistry, 2018, 57, 6561-6570.	4.0	40
51	3D-Graphene/Boron Nitride-stacking Material: a Fundamental van der Waals Heterostructure. Chemical Research in Chinese Universities, 2018, 34, 434-439.	2.6	7
52	Novel N–Br Bond-Containing <i>N</i> -Halamine Nanofibers with Antibacterial Activities. ACS Biomaterials Science and Engineering, 2018, 4, 2193-2202.	5.2	44
53	Certain doping concentrations caused half-metallic graphene. Journal of Saudi Chemical Society, 2017, 21, 111-117.	5.2	24
54	Fine-tuning π-spacer for high efficiency performance DSSC: A theoretical exploration with <mml:math <="" altimg="si1.gif" td="" xmlns:mml="http://www.w3.org/1998/Math/MathML"><td>مم³.7</td><td>49</td></mml:math>	مم ³ .7	49

overflow="scroll"><mml:mrow><mml:mi>D</mml:mi><mml:mo>â³</mml:mo>î⁴</mml:mi>ï€</mml:mi><mml:mi><mml:mo>â³</mml:mi>based organic dye. Dyes and Pigments, 2017, 141, 251-261.

Ran Jia

#	Article	IF	CITATIONS
55	The effect of relative position of the π -spacer center between donor and acceptor on the overall performance of D- π -A dye: a theoretical study with organic dye. Electrochimica Acta, 2017, 241, 440-448.	5.2	27
56	Theoretical study on hydrogen storage capacity of expanded h-BN systems. Computational Materials Science, 2017, 139, 335-340.	3.0	32
57	Novel Carbon Nanotubes Rolled from 6,6,12-Graphyne: Double Dirac Points in 1D Material. Journal of Physical Chemistry C, 2017, 121, 14835-14844.	3.1	28
58	The effect of D–[D _e –π–A] _n (n = 1, 2, 3) type dyes on the overall performance of DSSCs: a theoretical investigation. Journal of Materials Chemistry C, 2017, 5, 7510-7520.	5.5	22
59	Anionic ancillary ligands in cyclometalated Ru(<scp>ii</scp>) complex sensitizers improve photovoltaic efficiency of dye-sensitized solar cells: insights from theoretical investigations. Journal of Materials Chemistry A, 2017, 5, 15567-15577.	10.3	33
60	The influence of a dye–TiO ₂ interface on DSSC performance: a theoretical exploration with a ruthenium dye. RSC Advances, 2016, 6, 81976-81982.	3.6	28
61	DFT/TD-DFT calculations on the sensing mechanism of a dual response near-infrared fluorescent chemosensor for superoxide anion and hydrogen polysulfides: photoinduced electron transfer. RSC Advances, 2016, 6, 104735-104741.	3.6	23
62	Why HSâ^' and CNâ^' can be detected by different chemosensors with similar structures: a quantum mechanics and molecular dynamics study. RSC Advances, 2016, 6, 63548-63558.	3.6	2
63	From determination of the fugacity coefficients to estimation of hydrogen storage capacity: A convenient theoretical method. International Journal of Hydrogen Energy, 2015, 40, 10908-10917.	7.1	11
64	Exploring the sensitization properties of thienyl-functionalized tripyrrole Ru(II) complexes on TiO2 (101) surface: a theoretical study. Theoretical Chemistry Accounts, 2015, 134, 1.	1.4	7
65	Theoretical studies on the spectroscopic properties of porphyrin derivatives for dye-sensitized solar cell application. RSC Advances, 2015, 5, 33653-33665.	3.6	30
66	Theoretical studies on the absorption spectra and intramolecular charge transfer of push-pull zinc porphyrin dyes for dye-sensitized solar cells. Chemical Research in Chinese Universities, 2015, 31, 276-280.	2.6	6
67	Investigation of Properties of Mg _{<i>n</i>} Clusters and Their Hydrogen Storage Mechanism: A Study Based on DFT and a Global Minimum Optimization Method. Journal of Physical Chemistry A, 2015, 119, 3636-3643.	2.5	40
68	What Makes Hydroxamate a Promising Anchoring Group in Dye-Sensitized Solar Cells? Insights from Theoretical Investigation. Journal of Physical Chemistry Letters, 2014, 5, 3992-3999.	4.6	61
69	The correlations among the fragility of supercooled liquids, the fragility of superheated melts, and the glass-forming ability for marginal metallic glasses. Journal of Applied Physics, 2009, 105, 024304.	2.5	11